Geophysical Research Letters

RESEARCH LETTER
10.1029/2020GL088944

Continuous Dissolved Gas Tracing of Fracture-Matrix Exchanges

R. Hoffmann[1,2], P. Goderniaux[2], P. Jamin[1], E. Chatton[3], J. de la Bernardie[3], T. Labasque[3], T. Le Borgne[3], and A. Dassargues[1]

[1]Hydrogeology and Environmental Geology, UEE, Liège University, Liège, Belgium, [2]Geology and Applied Geology, Polytech Mons, University of Mons, Mons, Belgium, [3]Geoscience Rennes, University Rennes 1, Rennes, France

Key Points:
- Multitracer tests were performed in a fractured chalk aquifer using continuously monitored solute and dissolved gas tracers
- The different molecular diffusion coefficients of dissolved gas tracers provide new information on fracture-matrix exchanges
- A methodology is presented to invert peak time, peak intensity, and tailing slope to quantify fracture-matrix exchanges

Supporting Information:
- Supporting Information S1

Correspondence to:
R. Hoffmann,
richard.hoffmann@uliege.be

Citation:
Hoffmann, R., Goderniaux, P., Jamin, P., Chatton, E., de la Bernardie, J., Labasque, T., et al. (2020). Continuous dissolved gas tracing of fracture-matrix exchanges. *Geophysical Research Letters*, *47*, e2020GL088944. https://doi.org/10.1029/2020GL088944

Received 19 MAY 2020
Accepted 12 AUG 2020
Accepted article online 21 AUG 2020

Abstract Transport in fractured media plays an important role in a range of processes, from rock weathering and microbial processes to contaminant transport, and energy extraction and storage. Diffusive transfer between the fracture fluid and the rock matrix is often a key element in these applications. But the multiscale heterogeneity of fractures renders the field assessment of these processes extremely challenging. This study explores the use of dissolved gases as tracers of fracture-matrix interactions, which can be measured continuously and highly accurately using mobile mass spectrometers. Since their diffusion coefficients vary significantly, multiple gases are used to probe different scales of fracture-matrix exchanges. Tracer tests with helium, xenon, and argon were performed in a fractured chalk aquifer, and resulting tracer breakthrough curves are modeled. Results show that continuous dissolved gas tracing with multiple tracers provides key constrains on fracture-matrix interactions and reveal unexpected scale effects in fracture-matrix exchange rates.

Plain Language Summary Fractures provide pathways to flow, chemical elements and energy, as well as habitats for microorganisms in the Earth's subsurface. Due to diffusion and reaction, dissolved chemical elements are continuously exchanged between groundwater flowing in the fractures and the surrounding rock matrix. This process exerts a strong influence on many biogeochemical processes. Yet, due to multiscale heterogeneity of fracture systems, the characterization of fracture-matrix interactions is challenging and there is high uncertainty on relevant conceptual models. This study explores the use of dissolved gases as tracers of fracture-matrix interactions. Their larger diffusion coefficients compared to classical tracers allow a deeper penetration into the matrix compared to conventional fluorescent dyes, and recent field mass spectrometers allow a continuous and highly accurate monitoring. Field tracer test results are interpreted with mathematical models, providing new constraints on the definition and parametrization of transport models in fractured rocks.

1. Motivation

As pathway for fluid flow and the transport of matter and energy in the subsurface, fractures play a central role in a broad range of Earth processes, including rock weathering (Riebe et al., 2017; St. Clair et al., 2015), subsurface microbial processes (Bochet et al., 2020; Li et al., 2017; Lima et al., 2018), contaminant transport (Bear et al., 1993; Berkowitz et al., 1988; Berkowitz & Scher, 1996; Bibby, 1981; Neuman, 2005; Parker et al., 1994), or energy extraction and storage (Klepikova et al., 2016; Lee, 2010; Read et al., 2013). The characterization and modeling of transport processes in fractured environment is particularly challenging due to the extreme heterogeneity of flow rates and transport time scales (Blessent et al., 2014; Kang et al., 2015; Tsang, 1995; Weatherill et al., 2008). Preferential flow in fracture networks promotes fast transfers, while diffusion from the fractures into the rock matrix can lead to very long residence times (Becker & Shapiro, 2000, 2003; Haggerty et al., 2000; Hyman et al., 2019; Kang et al., 2015; Le Borgne & Gouze, 2008; Parker et al., 2010).

Due to their multiscale nature (Berkowitz et al., 2000; Bonnet et al., 2001), the characterization of flow and transport in fractured rocks is extremely challenging (Bear et al., 1993; Brouyère et al., 2000; Jenabidehkordi, 2018; Le Borgne et al., 2006; Tsang & Neretnieks, 1998; Van den Daele et al., 2007). A common hydrogeological practice is to perform solute tracer tests using dye or salt tracer fluids, which provide information on transfer times and dispersion processes (Barker, 2010; Becker & Shapiro, 2000; Brouyère et al., 2005;

Brouyère & Dassargues, 2002; Chen et al., 2007; Dorn et al., 2011; Labat & Mangin, 2015; Maliva, 2016; Raven et al., 1988; Shakas et al., 2017; Singhal & Gupta, 2010; Tsang & Neretnieks, 1998). However, based on common tracer tests results, it is generally difficult to converge to a unique characterization of transport dynamics in terms of geometry and parameterization (Carrera et al., 2005; Maliva, 2016; Singhal & Gupta, 2010). In heterogeneous media, inverse modeling of solute breakthrough curves is often an ill-posed problem, and large dispersive coefficients are often used to counterbalance deficiencies in the model conceptualization and correlations between parameters (Carrera et al., 2005; Davis et al., 1980; Maliva, 2016; Renard, 2007; Singhal & Gupta, 2010).

The signature of fracture-matrix exchanges on tracer breakthrough curves is a strong late-time tailing, characterized by a power law decay of late time concentrations (Haggerty et al., 2000; Haggerty & Gorelick, 1995; Hyman et al., 2019; Kirchner et al., 2000; Maloszewski & Zuber, 1993; Małoszewski & Zuber, 1985; Tsang, 1995; Weede & Hötzl, 2005). For idealized parallel plate fractures and a homogeneous matrix, the expected late time decay is $(t) \sim t^{-b}$, with $b = 1.5$ (Carrera et al., 1998; Haggerty et al., 2000). However, a broad range of power law exponents b have been observed, depending on the context, and significance in terms of flow heterogeneity within preferential flowpaths and multiple rates of mass transfer in the matrix is still debated and difficult to assess (Becker & Shapiro, 2003; Carrera et al., 1998; Dentz & Berkowitz, 2003; Gouze, Le Borgne, et al., 2008; Gouze et al., 2008; Haggerty et al., 2001; Hyman et al., 2019; Kang et al., 2015; Le Borgne & Gouze, 2008). The use of tracers with multiple diffusion coefficients (Becker & Shapiro, 2000) and combining different forced gradient configurations such as convergent and push-pull (Becker & Shapiro, 2003; Kang et al., 2015) have been shown to considerably reduce the uncertainty for the inference of relevant transport physics from tracer tests. But the range of diffusion coefficients of fluorescent dyes that can be continuously monitored in situ is limited, and other solute tracers require heavy sampling and analysis. To overcome these challenges, this study investigates the potential of in situ continuous dissolved gas tracing to quantify fracture-matrix interactions.

The potential use of dissolved gases as tracers in groundwater studies was established around 20 years ago (Sanford et al., 1996; Solomon et al., 1998). Due to their higher molecular diffusion coefficients, interactions of dissolved gases (e.g., $D = 58.8 \times 10^{-10}$ m^2 s^{-1} for helium 12°C; Jähne et al., 1987) with the rock matrix are stronger compared to classical tracers (e.g., $D = 4.5 \times 10^{-10}$ m^2 s^{-1} for uranine; Skagius & Neretnieks, 1986). Sanford et al. (2002) combined bromide ($D = 25 \times 10^{-10}$ m^2 s^{-1}) and helium in a tracer test performed in fractured rock to calibrate a fracture-matrix model. Although uncertainty was large due to low mass recovery, the larger diffusion coefficient of helium was shown to delay and dilute the breakthrough curve peak compared to bromide, highlighting the effect of matrix diffusion. While these early dissolved gas studies relied on field sampling and laboratory measurements, the recent development of portable mass spectrometer now allows on-site continuous measurements of multiple gas tracers with high accuracy (Brennwald et al., 2016; Chatton et al., 2017). Innovative techniques based on membrane inlet mass spectrometry (MIMS) enable the in situ measurement of reactive and noble dissolved gases in oceanic and continental waters (Bell et al., 2007; Brennwald et al., 2016; Camilli & Hemond, 2004; Cassar et al., 2009; Chatton et al., 2017; Mächler et al., 2012; Roques et al., 2020; Tortell, 2005).

Here we explore the potential of this technology in active mode. Forced gradient tracer test experiments were performed in a dual porosity porous/fractured chalk aquifer using helium, argon, and xenon as dissolved gases and uranine as fluorescent dye, characterized by diffusion coefficients of in total one order of magnitude difference. After transport in the fracture network, tracer recovery was measured continuously on-site using a portable mass spectrometer for dissolved gases and a fluorimeter for uranine. This technique first allows the possible measurement of multiple tracers with different diffusion coefficients probing different time scales of fracture-matrix interactions. Second, the high accuracy of measurements at low concentration allows a fine analysis of the late time breakthrough curve tailing, which provides critical information on the physics of fracture-matrix exchanges. Using analytical solutions of tracer transport in fractures and diffusion into the matrix, the study shows that continuous high accuracy measurement of tracers of different diffusion coefficients allows inferring unexpected transport dynamics in fracture-matrix systems.

2. Methods and Data

2.1. Test Site and Tracer Properties

Injection of a fluorescent dye tracer (uranine) jointly with dissolved gases was performed in a fractured chalk aquifer (supporting information Text S1 and Figure S1). This aquifer is considered as a typical dual porosity, dual permeability reservoir with a total porosity of the porous matrix estimated to about 40%, including about 1% of fractures (Batlle Aguilar et al., 2007; Brouyère, 2001; Dassargues, 2018; Goderniaux et al., 2018; Rorive & Goderniaux, 2014). While fractures allow fast preferential flows and explain most of the aquifer transmissivity, the matrix porosity is characterized by a lower hydraulic conductivity but enables the storage of large quantities of groundwater (Dassargues, 2018; Dassargues & Monjoie, 1993; Downing et al., 1993).

The diffusion coefficients of the used tracers vary over one order of magnitude, where helium has the highest (58.8×10^{-10} m^2 s^{-1}), argon and xenon have an intermediate one (21.1×10^{-10} m^2 s^{-1} and 9.9×10^{-10} m^2 s^{-1}, respectively), and uranine as dye tracer has the lowest one (4.5×10^{-10} m^2 s^{-1}). Background concentrations of uranine, helium, and xenon in the aquifer are low (6.50×10^{-7} g L^{-1}, 1.67×10^{-9} mol L^{-1}, and 4.30×10^{-10} mol L^{-1}, respectively), while for argon, one of the major dissolved gases in natural waters, it is 1.73×10^{-5} mol L^{-1}.

2.2. CF-MIMS—Dissolved Gas Measurement

A membrane inlet mass spectrometry (MIMS) technique is used for monitoring dissolved gas concentration on-site. For this purpose, an EQuilibrium (EQ-) Membrane system (Brennwald et al., 2016) or a Continuous Flow (CF-) Membrane Inlet Mass Spectrometer (MIMS) is suitable (Chatton, 2017; Chatton et al., 2017). The system uses an inlet system developed to enhance its sensitivity and response time to "light" gases (<50 amu especially <20 amu), and previous tests showed that this selectivity has a price for "heavy" gases (>100 amu) which sensitivity decrease and response times increase with the gas mass. Response times are typically below 30 s for light gases and reach up to a few minutes for detectable heavy gases. In this study, the heavy gas xenon is therefore affected by a delay in measurements changing the amplitude for small observation times, while the light gases argon and helium are not affected. With more time, these effects are less significant, so that the tailing of xenon can be still used.

2.3. Experimental Setup

The two wells Pz1 and Pz2 (distant 7.55 m) are connected by open horizontal fractures, and two experiments were performed with joint injections of dissolved gases and uranine in a single fracture located at 34.8 m deep in Pz2, using an inflatable double packer system: (1) a convergent forced gradient experiment with recovery in Pz1 and (2) a push-pull experiment in Pz2 (Figure S1). In the convergent experiment, 89.46 L of water, containing 2.0 g of uranine, were partially saturated with helium, xenon, and argon corresponding to concentrations of 2.0×10^{-5} mol L^{-1} (0.007 g), 1.7×10^{-5} mol L^{-1} (0.20 g), and 1.8×10^{-3} mol L^{-1} (6.37 g), respectively. All tracers were injected jointly in Pz2 at a flow rate of 0.57 m^3 hr^{-1} and extracted continuously in Pz1, at a constant flow rate of 7.2 m^3 hr^{-1}. Uranine and dissolved gases were continuously measured using a field fluorimeter and the CF-MIMS, respectively. In the push-pull experiment, 92.63 L of water, containing 0.2 g of uranine, were partially saturated with helium, xenon, and argon corresponding to concentrations of 2.7×10^{-5} mol L^{-1} (0.01 g), 9.0×10^{-6} mol L^{-1} (0.11 g), and 6.4×10^{-4} mol L^{-1} (2.2 g). All tracers were injected jointly in Pz2 at a flow rate of 0.57 m^3 hr^{-1}, followed by a "resting time" period of 0.33 hr, and a pumping period of 19.70 hr in the isolated fracture at the same flow rate than injection. Pumped water is continuously conveyed to the CF-MIMS and a field fluorimeter for continuous analysis. During this experiment, no pumping is operated in Pz1.

2.4. Breakthrough Curves Normalization

Measured breakthrough curves are normalized by the integrated concentration, which provides a residence time distribution (RTD) p(t) (s^{-1}), as described by Equation 1 (Becker & Shapiro, 2000; Raven et al., 1988):

$$p(t) = \frac{C(t)}{\int_0^\infty C(t)\,dt} \quad (1)$$

where C(t) is the concentration measured at time t (s) in the recovery well.

3. Results and Discussion

3.1. Analysis of Peak Time and Concentration

In the convergent test, the peak times increase, and the normalized peak values decrease with increasing diffusion coefficient (Figures 1a, 3a, 3c, and 3e and Table 1). For example, compared to uranine, the helium breakthrough is 35% more diluted and has a 15% larger peak time (Figure 1a). The peak time of xenon, a heavy gas, is however delayed, compared to the other light gases (Figure 1a) as discussed in section 2.2.

For the push-pull test, the tracer peak times decrease with increasing molecular diffusion coefficients (Figures 1b, 3b, 3d, and 3f and Table 1). For example, the peak time value of uranine (0.76 hr) is delayed of 5% compared to helium (0.72 hr). As in the convergent test, xenon is delayed (11% and 5% compared to helium and uranine, respectively) (Figure 1b). The trend of the normalized peak values is less clear, and helium and xenon values are unexpectedly high, compared with uranine and argon (Figures 1a, 1b, and 3f and Table 1). Note however that some uncertainty affecting these values may arise from background concentration estimation issues related to remnant tracer from previous experiments. Measured xenon concentration values are also characterized by some visible oscillations, due to strong night and day temperature variations affecting the accuracy of measurements and the assessment of the background for the push-pull experiment.

The different trends observed for peak time and amplitude in convergent and push-pull tests may be understood as follows. For the convergent test, an increasing diffusion coefficient leads to enhanced exchange with the matrix leading to both delayed peak time and smaller peak amplitude (Sanford et al., 2002). For the push-pull test, increasing the diffusion coefficient enhances solute diffusion into the rock matrix and limits transport of the tracer from the injection point to the fracture network. In the pull phase, a larger mass of tracer is close to the injection point, and therefore the peak time decreases with the diffusion coefficient, as shown by Klepikova et al. (2016) for heat diffusion. The peak amplitude decays with diffusion coefficient like in the convergent test, due to enhanced diffusion. In the following, these trends are confirmed from analytical solutions.

3.2. Analysis of Late-Time Tailing

Late time tailing could be analyzed with high precision for helium and uranine, while xenon and argon were affected by the resolution limit (Figure 1c). In the case of xenon, the background measurements are fluctuating around 4×10^{-10} mol L^{-1}, which is a too low-resolution limit for accurate late time tailing observations (Text S1 and Figures S2 to S4). As argon is one of the major dissolved gas in waters and the tracer injection amount is limited, it remains difficult to induce a contrast which is large enough (Figure S2).

Helium and uranine display power law behavior both for the convergent and push-pull tests. The exponent value is calculated considering concentration values where the slope is constant (from 2.5 to 36 hr for the convergent test and from 6 to 16 hr for the push-pull tests). For the convergent test, the tailing of helium has a significantly lower exponent ($b = 1.10$) compared to uranine ($b = 1.53$) (Figure 1c). In the push-pull test, the late time tailing of helium and uranine is similar (Figure 1d) and characterized by an exponent approximately equal to $b = 1.5$ (Table 1).

The exponent $b = 1.5$ is typical of diffusion perpendicular to a planar fracture into the adjacent rock matrix (Haggerty et al., 2000). So all measured late time tailings except for helium in the convergent test suggest the relevance of a simple model of fracture-matrix exchange. However, the convergent test tailing of helium, the tracer with the largest diffusion coefficient, is significantly different ($b = 1.10$). Klepikova et al. (2016) showed that for highly channelized flow, diffusion from fractures to matrix becomes radial instead of effectively one-dimensional for the parallel plate model. This leads to a late time tailing as $c(t) \sim t^{-1}/\log(t^2)$, which is close to $c(t) \sim t^{-1}$. Hence, the late time tailing of helium suggests that tracers that penetrate more deeply into the matrix are influenced by a radial diffusion behavior, possibly indicating strong channeling of flow

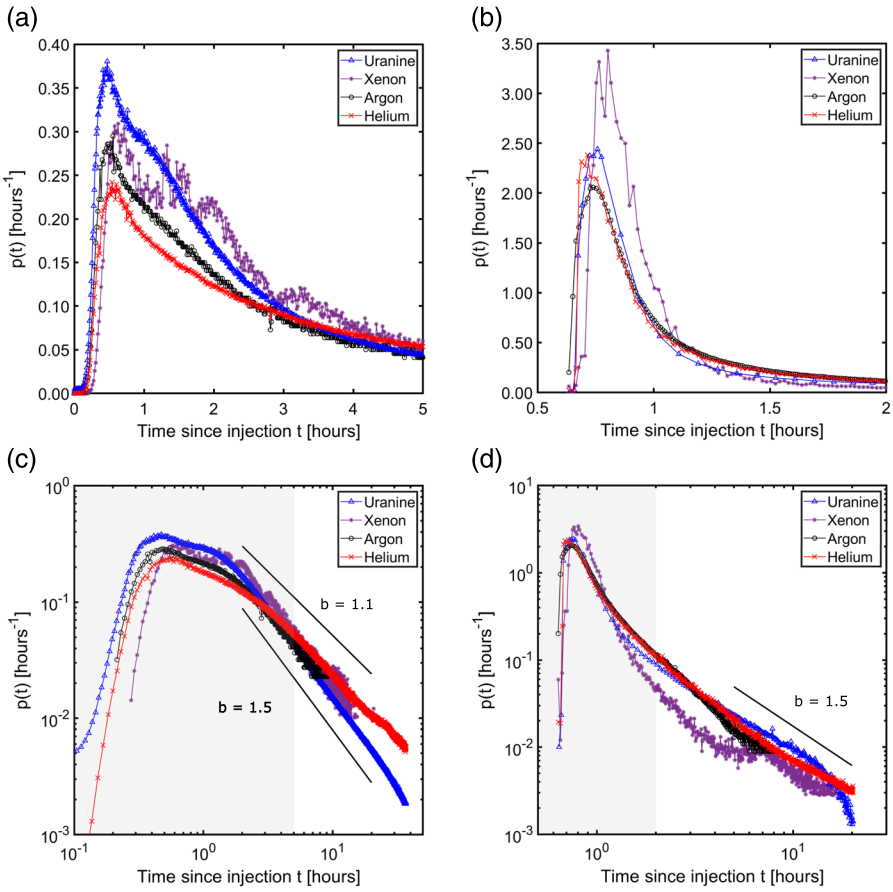

Figure 1. Zoom of uranine, helium, xenon, and argon breakthrough curves peak in linear scale for (a) the convergent and (b) push-pull experiment. Full breakthrough curves in log-log scale for (c) the convergent and d the push-pull experiment. The gray "transparent" in (c) and (d) corresponds to the zoomed section of (a) and (b). Tracers are listed in the legend by ascending diffusion coefficient (Table 1).

in fractures. Over the experimental time (39 hr), the characteristic scale of penetration of uranine into the matrix is 2 cm, while that of helium is 7 cm. In the investigated aquifer, fractures are regionally observed in outcropping chalks, including numerous bedding joints, each of them being characterized by a highly variable aperture, inducing channelization of flow. Based on that, it is hypothesized that for small matrix penetration depths, solutes only probe the fringes bordering the channels. At this scale, the effect of larger-scale channels may be negligible and mass transfer may be effectively perpendicular to the local

Table 1
Overview of the main tracing results, when injecting a dissolved gas cocktail jointly with uranine in convergent and push-pull configuration into a double porous chalk aquifer

Set up	Tracer	Aqueous diffusion coefficient 12°C ($m^2\ s^{-1}$)		Recovered (%)	Peak value (hr^{-1})	Peak time (hr)	Slope b (–)	95% interval (–)
Convergent 89.46 L	Uranine	$4.50 \cdot 10^{-10}$	(Skagius & Neretnieks, 1986)	81.4	0.38	0.47	1.53	1.528; 1.531
Injected (+45 L flush)	Xenon	$9.91 \cdot 10^{-10}$	(Jähne et al., 1987)	95.8	0.31	0.63	—	—
	Argon	$21.10 \cdot 10^{-10}$	(Chatton, 2017)	99.6	0.29	0.49	—	—
	Helium	$58.80 \cdot 10^{-10}$	(Chatton, 2017; Jähne et al., 1987)	99.5	0.24	0.54	1.10	1.097; 1.102
Push-pull 92.63 L	Uranine	See above		98.0	2.44	0.76	1.41	1.291; 1.535
Injected (+45 L flush)	Xenon			95.7	3.43	0.80	—	—
	Argon			97.5	2.06	0.74	—	—
	Helium			97.6	2.38	0.72	1.55	1.529; 1.562

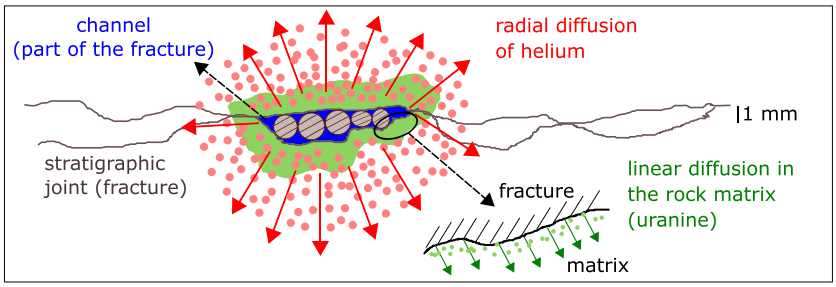

Figure 2. Schematic explanation of the different behavior of helium and uranine. At the small scale sampled by uranine, matrix diffusion is locally perpendicular to the surface and behaves effectively like the parallel plate model. At the larger scale sampled by helium, the presence of macroscopic channels leads to radial diffusion in the matrix, captured by the channel model.

fracture-rock interface (Figure 2). At larger penetration depths, it is likely that the effect of radial diffusion from channels starts to influence fracture-matrix mass transfer (Figure 2).

The change of tailing exponent with tracer diffusion is not observed for the push-pull tests. This may be due to the smaller involved rock volumes, time intervals, and distances in the push-pull experiment. The characteristic scale of the convergent test may be estimated as the distance between the boreholes $d = 7.55$ m. It is significantly smaller for the push-pull test where it is estimated as the average radius of injected fluid around the injection point, $r = (3V/4\varphi\pi)^{1/3}$, with V the total injected volume. This radius remains below 1.4 m if considering a minimum porosity φ of 1% (Table 1). Note however that the uncertainty related to the tailing exponent calculation is higher for this push-pull experiment than for the convergent test. This is mainly due to the combined challenge related to the duration of the monitoring after the peak time and the correct evaluation of the background concentration, which was here influenced by previous experiments and not strictly constant during the push-pull monitoring, affecting the normalization and slope calculation procedures.

3.3. Breakthrough Curve Modeling

The analysis of peak time and amplitude, as well as late time tailing provides some qualitative insights into the transport dynamics and fracture-matrix interactions. To extract quantitative information on these dynamics, we interpreted the breakthrough curves with analytical solutions of advection and dispersion in fractures and diffusion into the matrix. Following the observations of breakthrough curve tailing, two different conceptual models for the fracture geometry are tested: the parallel plate model and the channel model (Figure S5). The analytical solutions described by De La Bernardie (2018) and De La Bernardie et al. (2018, 2019) based on Laplace transforms (Text S2) are used. These Laplace transform solutions are inverted using the algorithms from Hoog et al. (1982) and Hollenbeck (1998). Manual parameter adjustments are simultaneously operated on the experimental uranine and helium breakthrough curves in RTD using Equation 1 and considering equal weight on the peak value, peak time, and slope in RTD and minimizing the difference between observations and simulations according to the diffusion coefficient (Figure 3).

Optimized parameters include the number of fractures or channels, the fracture aperture or channel radius, and the dispersivity in fractures/channels.

As expected from the different power law tailing exponents of the uranine and helium breakthrough curves in the convergent tracer test (Figure 1c), the uranine breakthrough curve is well captured by the parallel plate model, while the helium breakthrough curve is well captured by the channel model. The uranine breakthrough curve is simulated using $n_f = 40$ fractures with an aperture $a = 1$ mm and a dispersivity of $\alpha = 2.4$ m. The helium recovery is simulated using $n_c = 700$ channels characterized by a radius of $a = 1$ mm and a dispersivity of $\alpha = 1.5$ m. This suggests that, in the area sampled by the tracer, fractures contained on average 17 channels per fracture. Using the parallel plate model for the uranine breakthrough curve, fails to predict the helium breakthrough curve and vice versa (Text S4 and Figure S10), which confirms the transition in the fracture-matrix interaction mode with different tracer penetration depths into the matrix. This transition tends to be confirmed by the modeling of peak

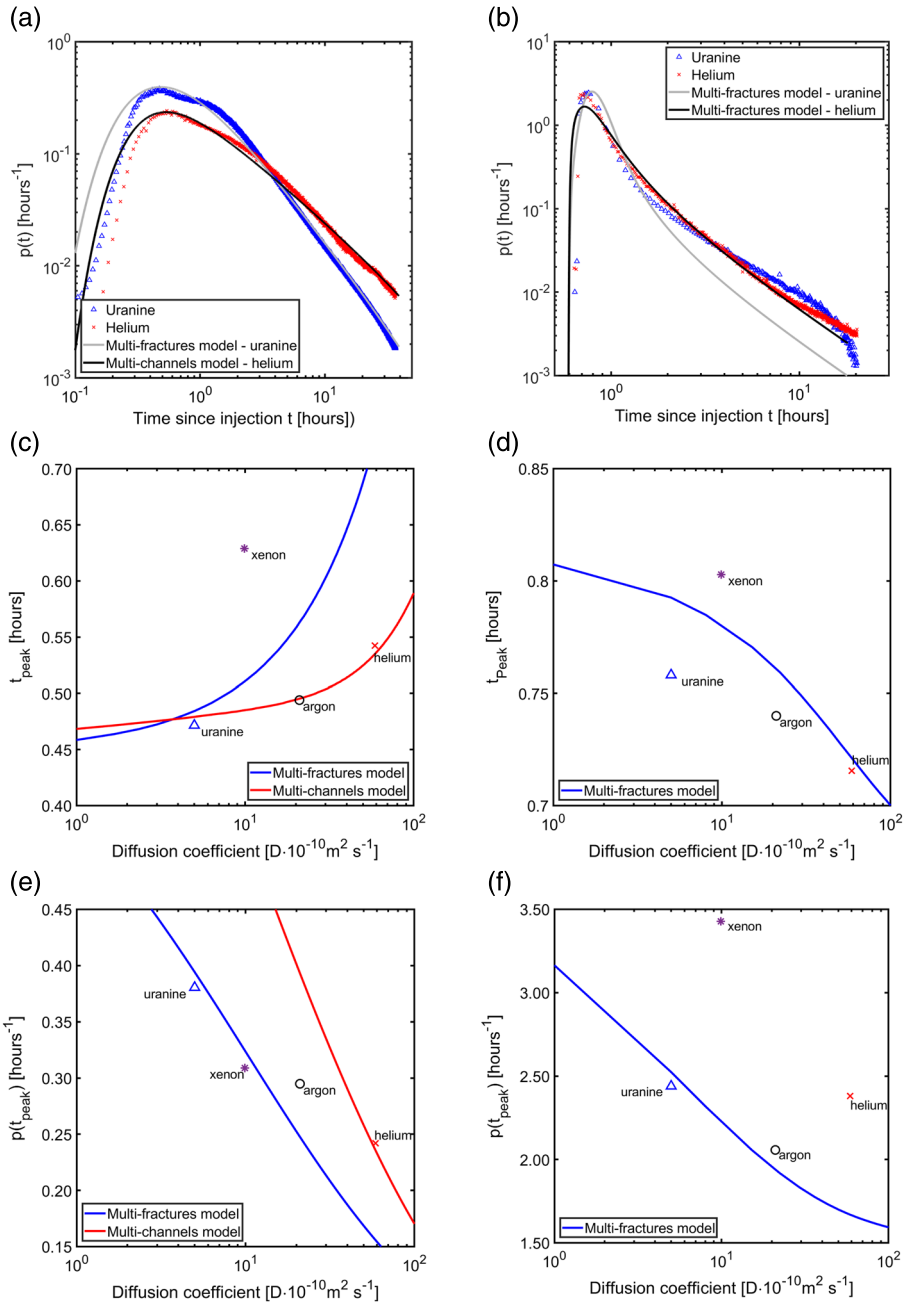

Figure 3. Modeling of the (a) convergent and (b) push-pull experiment for uranine and helium. Peak times of the (c) convergent and (d) push-pull configuration, and peak values in RTD for (e) convergent and (f) push-pull configuration in the parameter adjustment. Tracers are listed in the legend by ascending diffusion coefficient (Table 1).

time and amplitude, which shows a transition from the parallel plate trend to the channel trend (Figures 3c and 3e). As discussed in Text S3 and in Figures S6 to S9, the dependency of the peak time and amplitude on the diffusion coefficient shows a strong sensitivity to model parameters. Hence, the analysis of the dependency of peak time and amplitude on the diffusion coefficient offers an alternative way to characterize the dynamics of fracture-matrix interactions.

Push-pull experiments are generally consistent with the parallel plate fracture model, which successfully captures the uranine and helium breakthrough curves with a single set of parameters (Figure 3b). Note that the slight mismatch for the tailing of uranine may be due to more uncertain background concentrations

related to previous convergent experiment. The best fit aperture is a = 1 mm, as for the convergent test. The number of fractures for the best fit model was 4, that is, much less than for the convergent test, which reflects the much smaller rock volume investigated by the push-pull test. The best fit dispersivity was $\alpha = 0.1$ m, which is much lower than for the convergent test. This is consistent with the fact that a large part of dispersion, the reversible dispersion, is canceled in push-pull tests (Kang et al., 2015). The model also captures the dependency of the peak time and peak value to the diffusion coefficient, although the trend is less clear for the peak (Figures 3d and 3f).

4. Conclusions

In this study, we have explored the use of continuously monitored dissolved gases as tracers of fracture-matrix interactions using recently developed field mass spectrometers. Highly accurate measurements at low concentrations allowed for a refined analysis of late time breakthrough curve tailing, a key for capturing the physics of fracture-matrix interactions and bringing new insights about the debate on power law decay. The experimental results suggested that the model derived from a conventional fluorescent dye, with relatively low matrix penetration depth, could not be used to predict the transport behavior of helium, characterized by a deeper penetration depth into the matrix. The study showed that the effects of channeled fracture flow started to be dominant at larger scales, highlighting the challenge to describe the scale dependency of fracture-matrix interactions and the interest of using tracers of different diffusion coefficients for conceptual model definition.

Tracer tests results bring complimentary data supporting the reconstruction of the porous/fractured medium. Interpretation with analytical solutions showed that these innovative data are sensitive to hydraulic and geometrical parameters, which are also better constrained in comparison with classical experiments. Results thus support characterization and further modeling of dual media toward more robust simulations and predictions.

Data Availability Statement

Data sets analyzed for this study are stored on the H+ Network database (http://hplus.ore.fr/en/hoffmann-et-al-2020-grl-data).

Acknowledgments

The ITN ENIGMA has received funding from European Union's Horizon 2020 research and innovation programme under the Marie Sklodowska-Curie Grant Agreement 722028. The Belgian "Fonds de la Recherche Scientifique"—FNRS under Grant J.0115.15 founded part of the test site. Most of the equipment, especially the CF-MIMS and Mobile lab, were funded by the CRITEX project (ANR-11-EQPX-0011). Analyses with μGC and MIMS were performed within the CONDATE EAU analytical platform in Rennes (https://condate-eau.univ-rennes1.fr/). The authors express their special thanks to B. Deletter, C. Barcella, H. E. Hoffmann, A. Battais, N. Guihéneuf, and two anonymous reviewers.

References

Barker, J. A. (2010). Modelling doublets and double porosity. *Quarterly Journal of Engineering Geology and Hydrogeology*, *43*(3), 259–268. https://doi.org/10.1144/1470-9236/08-095

Batlle Aguilar, J., Orban, P., Dassargues, A., & Brouyère, S. (2007). Identification of groundwater quality trends in a chalk aquifer threatened by intensive agriculture in Belgium. *Hydrogeology Journal*, *15*(8), 1615–1627. https://doi.org/10.1007/s10040-007-0204-y

Bear, J., Tsang, C.-F., & de Marsily, G. (1993). *Flow and contaminant transport in fractured rock* (1st ed.). San Diego, CA: Academic Press. https://doi.org/10.1016/C2009-0-29127-6

Becker, M. W., & Shapiro, A. M. (2000). Tracer transport in fractured crystalline rock: Evidence of nondiffusive breakthrough tailing. *Water Resources Research*, *36*(7), 1677–1686. https://doi.org/10.1029/2000WR900080

Becker, M. W., & Shapiro, A. M. (2003). Interpreting tracer breakthrough tailing from different forced-gradient tracer experiment configurations in fractured bedrock. *Water Resources Research*, *39*(1), 1024. https://doi.org/10.1029/2001WR001190

Bell, R. J., Short, R. T., van Amerom, F. H. W., & Byrne, R. H. (2007). Calibration of an in situ membrane inlet mass spectrometer for measurements of dissolved gases and volatile organics in seawater. *Environmental Science & Technology*, *41*(23), 8123–8128. https://doi.org/10.1021/es070905d

Berkowitz, B., Bear, J., & Braester, C. (1988). Continuum models for contaminant transport in fractured porous formations. *Water Resources Research*, *24*(8), 1225–1236. https://doi.org/10.1029/WR024i008p01225

Berkowitz, B., Bour, O., Davy, P., & Odling, N. (2000). Scaling of fracture connectivity in geological formations. *Geophysical Research Letters*, *27*(14), 2061–2064. https://doi.org/10.1029/1999GL011241

Berkowitz, B., & Scher, H. (1996). Influence of embedded fractures on contaminant diffusion in geological formations. *Geophysical Research Letters*, *23*(9), 925–928. https://doi.org/10.1029/96GL00873

Bibby, R. (1981). Mass transport of solutes in dual-porosity media. *Water Resources Research*, *17*(4), 1075–1081. https://doi.org/10.1029/WR017i004p01075

Blessent, D., Jørgensen, P. R., & Therrien, R. (2014). Comparing discrete fracture and continuum models to predict contaminant transport in fractured porous media. *Groundwater*, *52*(1), 84–95. https://doi.org/10.1111/gwat.12032

Bochet, O., Bethencourt, L., Dufresne, A., Farasin, J., Pédrot, M., Labasque, T., et al. (2020). Iron-oxidizer hotspots formed by intermittent oxic–anoxic fluid mixing in fractured rocks. *Nature Geoscience*, *13*(2), 149–155. https://doi.org/10.1038/s41561-019-0509-1

Bonnet, E., Bour, O., Odling, N. E., Davy, P., Main, I., Cowie, P., & Berkowitz, B. (2001). Scaling of fracture systems in geological media. *Reviews of Geophysics*, *39*(3), 347–383. https://doi.org/10.1029/1999RG000074

Brennwald, M. S., Schmidt, M., Oser, J., & Kipfer, R. (2016). A portable and autonomous mass spectrometric system for on-site environmental gas analysis. *Environmental Science & Technology*, *50*(24), 13,455–13,463. https://doi.org/10.1021/acs.est.6b03669

Brouyère, S. (2001). *Study and quantification of contaminant transport and capturing in variably saturated underground media. Quantification of hydrodispersive parameters using field tracer techniques* (Doctoral dissertation). Liege, Belgium: University of Liege. Retrieved from http://hdl.handle.net/2268/40804

Brouyère, S., Carabin, G., & Dassargues, A. (2005). Influence of injection conditions on field tracer experiments. *Groundwater*, *43*(3), 389–400. https://doi.org/10.1111/j.1745-6584.2005.0041.x

Brouyère, S., & Dassargues, A. (2002). Reliability of transport models calibrated on field tracer experiments: Breakthrough curve sensitivity to tracer injection conditions. In K. Kovar, & Z. Hrkal (Eds.), *Calibration and reliability in groundwater modelling: A few steps closer to reality* (pp. 339–346). Wallingford: IAHS Press. Retrieved from http://hdl.handle.net/2268/3209

Brouyère, S., Dassargues, A., Therrien, R., & Sudicky, E. A. (2000). Modelling of dual porosity media: Comparison of different techniques and evaluation of the impact on plume transport simulations. In F. Stauffer, W. Kinzelbach, K. Kovar, & E. Hoehn (Eds.), *Calibration and reliability in groundwater modelling* (Vol. 265, pp. 22–27). Wallingford: IAHS Press. Retrieved from http://hdl.handle.net/2268/2803

Camilli, R., & Hemond, H. F. (2004). A mobile autonomous underwater mass spectrometer. *TrAC Trends in Analytical Chemistry*, *23*(4), 307–313. https://doi.org/10.1016/S0165-9936(04)00408-X

Carrera, J., Alcolea, A., Medina, A., Hidalgo, J., & Slooten, L. J. (2005). Inverse problem in hydrogeology. *Hydrogeology Journal*, *13*(1), 206–222. https://doi.org/10.1007/s10040-004-0404-7

Carrera, J., Sánchez-Vila, X., Benet, I., Medina, A., Galarza, G., & Guimerà, J. (1998). On matrix diffusion: Formulations, solution methods and qualitative effects. *Hydrogeology Journal*, *6*(1), 178–190. https://doi.org/10.1007/s100400050143

Cassar, N., Barnett, B. A., Bender, M. L., Kaiser, J., Hamme, R. C., & Tilbrook, B. (2009). Continuous high-frequency dissolved O_2/Ar measurements by equilibrator inlet mass spectrometry. *Analytical Chemistry*, *81*(5), 1855–1864. https://doi.org/10.1021/ac802300u

Chatton, E. (2017). *Contribution of dissolved gases to the understanding of groundwater hydrobiogeochemical dynamics* (Doctoral dissertation). Rennes, France: University of Rennes 1. Retrieved from https://tel.archives-ouvertes.fr/tel-01810743

Chatton, E., Labasque, T., de La Bernardie, J., Guihéneuf, N., Bour, O., & Aquilina, L. (2017). Field continuous measurement of dissolved gases with a CF-MIMS: Applications to the physics and biogeochemistry of groundwater flow. *Environmental Science & Technology*, *51*(2), 846–854. https://doi.org/10.1021/acs.est.6b03706

Chen, Y., Zhou, C., & Sheng, Y. (2007). Formulation of strain-dependent hydraulic conductivity for a fractured rock mass. *International Journal of Rock Mechanics and Mining Sciences*, *44*(7), 981–996. https://doi.org/10.1016/j.ijrmms.2006.12.004

Dassargues, A. (2018). *Hydrogeology—Groundwater science and engineering*. Boca Raton, FL: CRC Press. Retrieved from https://www.crcpress.com/Hydrogeology-Groundwater-Science-and-Engineering/Dassargues/p/book/9781498744003

Dassargues, A., & Monjoie, A. (1993). Belgium. In R. A. Downing, M. Price, & G. P. Jones (Eds.), *The hydrogeology of the chalk of North-West Europe* (pp. 153–169). Oxford: Oxford Science Publications.

Davis, S. N., Thompson, G. M., Bentley, H. W., & Stiles, G. (1980). Ground-water tracers—A short review. *Ground Water*, *18*(1), 14–23. https://doi.org/10.1111/j.1745-6584.1980.tb03366.x

De La Bernardie, J. (2018). *Modélisation et caractérisation expérimentale du transport de chaleur en milieu fracturé* (Doctoral dissertation). Rennes, France: University of Rennes 1. Retrieved from https://tel.archives-ouvertes.fr/tel-01799570/file/LA_BERNARDIE_Jerome_de.pdf

De La Bernardie, J., Bour, O., Guihéneuf, N., Chatton, E., Longuevergne, L., & Le Borgne, T. (2019). Dipole and convergent single-well thermal tracer tests for characterizing the effect of flow configuration on thermal recovery. *Geosciences*, *9*(10), 440–455. https://doi.org/10.3390/geosciences9100440

De La Bernardie, J., Bour, O., Le Borgne, T., Guihéneuf, N., Chatton, E., Labasque, T., et al. (2018). Thermal attenuation and lag time in fractured rock: Theory and field measurements from joint heat and solute tracer tests. *Water Resources Research*, *54*, 10,053–10,075. https://doi.org/10.1029/2018WR023199

Dentz, M., & Berkowitz, B. (2003). Transport behavior of a passive solute in continuous time random walks and multirate mass transfer. *Water Resources Research*, *39*(5), 1111. https://doi.org/10.1029/2001WR001163

Dorn, C., Linde, N., Le Borgne, T., Bour, O., & Baron, L. (2011). Single-hole GPR reflection imaging of solute transport in a granitic aquifer. *Geophysical Research Letters*, *38*, L08401. https://doi.org/10.1029/2011GL047152

Downing, R. A., Price, M., & Jones, G. P. (1993). *The hydrogeology of the chalk of north-west Europe*. Oxford: Oxford Science Publications.

Goderniaux, P., Beyek, A., Tchotchom, A., Poulain, A., Wattier, M.-L., & Vandycke, S. (2018). Study of the heterogeneity of hydraulic properties in a chalk aquifer unit, using sequential pumping and tracing experiments with packer systems. In J. A. Lawrence, M. Preene, U. L. Lawrence, & R. Buckley (Eds.), *Engineering in chalk: Proceedings of the chalk 2018 conference* (pp. 675–680). Scotland: ICE Virtual Library. https://doi.org/10.1680/eiccf.64072.675

Gouze, P., Le Borgne, T., Leprovost, R., Lods, G., Poidras, T., & Pezard, P. (2008). Non-Fickian dispersion in porous media: 1. Multiscale measurements using single-well injection withdrawal tracer tests. *Water Resources Research*, *44*, W12443. https://doi.org/10.1029/2007WR006278

Gouze, P., Melean, Y., Le Borgne, T., Dentz, M., & Carrera, J. (2008). Non-Fickian dispersion in porous media explained by heterogeneous microscale matrix diffusion. *Water Resources Research*, *44*, W11416. https://doi.org/10.1029/2007WR006690

Haggerty, R., Fleming, S. W., Meigs, L. C., & McKenna, S. A. (2001). Tracer tests in a fractured dolomite: 2. Analysis of mass transfer in single-well injection-withdrawal tests. *Water Resources Research*, *37*(5), 1129–1142. https://doi.org/10.1029/2000WR900334

Haggerty, R., & Gorelick, S. M. (1995). Multiple-rate mass transfer for modeling diffusion and surface reactions in media with pore-scale heterogeneity. *Water Resources Research*, *31*(10), 2383–2400. https://doi.org/10.1029/95WR10583

Haggerty, R., McKenna, S. A., & Meigs, L. C. (2000). On the late-time behavior of tracer test breakthrough curves. *Water Resources Research*, *36*(12), 3467–3479. https://doi.org/10.1029/2000WR900214

Hollenbeck, K. J. (1998). INVLAP.M: A Matlab function for numerical inversion of Laplace transforms by the de Hoog algorithm. Retrieved from http://www.isva.dtu.dk/staff/karl/invlap.htm

Hoog, F. R., Knight, J. H., & Stokes, A. N. (1982). An improved method for numerical inversion of Laplace transforms. *SIAM Journal on Scientific and Statistical Computing*, *3*(3), 357–366. https://doi.org/10.1137/0903022

Hyman, J. D., Rajaram, H., Srinivasan, S., Makedonska, N., Karra, S., Viswanathan, H., & Srinivasan, G. (2019). Matrix diffusion in fractured media: New insights into power law scaling of breakthrough curves. *Geophysical Research Letters*, *46*, 13,785–13,795. https://doi.org/10.1029/2019GL085454

Jähne, B., Heinz, G., & Dietrich, W. (1987). Measurement of the diffusion coefficients of sparingly soluble gases in water. *Journal of Geophysical Research*, *92*(C10), 10,767–10,776. https://doi.org/10.1029/JC092iC10p10767

Jenabidehkordi, A. (2018). Computational methods for fracture in rock: A review and recent advances. *Frontiers of Structural and Civil Engineering*, *13*, 273–287. https://doi.org/10.1007/s11709-018-0459-5

Kang, P. K., Borgne, T. L., Dentz, M., Bour, O., & Juanes, R. (2015). Impact of velocity correlation and distribution on transport in fractured media: Field evidence and theoretical model. *Water Resources Research*, *51*, 940–959. https://doi.org/10.1002/2014WR015799

Kirchner, J. W., Feng, X., & Neal, C. (2000). Fractal stream chemistry and its implications for contaminant transport in catchments. *Nature*, *403*(6769), 524–527. https://doi.org/10.1038/35000537

Klepikova, M. V., Le Borgne, T., Bour, O., Dentz, M., Hochreutener, R., & Lavenant, N. (2016). Heat as a tracer for understanding transport processes in fractured media: Theory and field assessment from multiscale thermal push-pull tracer tests. *Water Resources Research*, *52*, 5442–5457. https://doi.org/10.1002/2016WR018789

Labat, D., & Mangin, A. (2015). Transfer function approach for artificial tracer test interpretation in karstic systems. *Journal of Hydrology*, *529*(part 3), 866–871. https://doi.org/10.1016/j.jhydrol.2015.09.011

Le Borgne, T., Bour, O., Paillet, F. L., & Caudal, J.-P. (2006). Assessment of preferential flow path connectivity and hydraulic properties at single-borehole and cross-borehole scales in a fractured aquifer. *Journal of Hydrology*, *328*(1–2), 347–359. https://doi.org/10.1016/j.jhydrol.2005.12.029

Le Borgne, T., & Gouze, P. (2008). Non-Fickian dispersion in porous media: 2. Model validation from measurements at different scales. *Water Resources Research*, *44*, W06427. https://doi.org/10.1029/2007WR006279

Lee, K. S. (2010). A review on concepts, applications, and models of aquifer thermal energy storage systems. *Energies*, *3*(6), 1320–1334. https://doi.org/10.3390/en3061320

Li, L., Maher, K., Navarre-Sitchler, A., Druhan, J., Meile, C., Lawrence, C., et al. (2017). Expanding the role of reactive transport models in critical zone processes. *Earth-Science Reviews*, *165*, 280–301. https://doi.org/10.1016/j.earscirev.2016.09.001

Lima, P. L. T., Silva, M. L. N., Quinton, J. N., Batista, P. V. G., Cândido, B. M., & Curi, N. (2018). Relationship among crop systems, soil cover, and water erosion on a typic Hapludox. *Revista Brasileira de Ciência do Solo*, *42*, 1–16. https://doi.org/10.1590/18069657rbcs20170081

Mächler, L., Brennwald, M. S., & Kipfer, R. (2012). Membrane inlet mass spectrometer for the quasi-continuous on-site analysis of dissolved gases in groundwater. *Environmental Science & Technology*, *46*(15), 8288–8296. https://doi.org/10.1021/es3004409

Maliva, R. G. (2016). *Aquifer characterization techniques*. Cham: Springer International Publishing. https://doi.org/10.1007/978-3-319-32137-0

Małoszewski, P., & Zuber, A. (1985). On the theory of tracer experiments in fissured rocks with a porous matrix. *Journal of Hydrology*, *79*(3–4), 333–358. https://doi.org/10.1016/0022-1694(85)90064-2

Maloszewski, P., & Zuber, A. (1993). Tracer experiments in fractured rocks: Matrix diffusion and the validity of models. *Water Resources Research*, *29*(8), 2723–2735. https://doi.org/10.1029/93WR00608

Neuman, S. P. (2005). Trends, prospects and challenges in quantifying flow and transport through fractured rocks. *Hydrogeology Journal*, *13*(1), 124–147. https://doi.org/10.1007/s10040-004-0397-2

Parker, B. L., Chapman, S. W., & Cherry, J. A. (2010). Plume persistence in fractured sedimentary rock after source zone removal. *Ground Water*, *48*(6), 799–808. https://doi.org/10.1111/j.1745-6584.2010.00755.x

Parker, B. L., Gillham, R. W., & Cherry, J. A. (1994). Diffusive disappearance of immiscible-phase organic liquids in fractured geologic media. *Groundwater*, *32*(5), 805–820. https://doi.org/10.1111/j.1745-6584.1994.tb00922.x

Raven, K. G., Novakowski, K. S., & Lapcevic, P. A. (1988). Interpretation of field tracer tests of a single fracture using a transient solute storage model. *Water Resources Research*, *24*(12), 2019–2032. https://doi.org/10.1029/WR024i012p02019

Read, T., Bour, O., Bense, V., le Borgne, T., Goderniaux, P., Klepikova, M. V., et al. (2013). Characterizing groundwater flow and heat transport in fractured rock using fiber-optic distributed temperature sensing. *Geophysical Research Letters*, *40*, 2055–2059. https://doi.org/10.1002/grl.50397

Renard, P. (2007). Stochastic hydrogeology: What professionals really need? *Ground Water*, *45*(5), 531–541. https://doi.org/10.1111/j.1745-6584.2007.00340.x

Riebe, C. S., Hahm, W. J., & Brantley, S. L. (2017). Controls on deep critical zone architecture: A historical review and four testable hypotheses. *Earth Surface Processes and Landforms*, *42*(1), 128–156. https://doi.org/10.1002/esp.4052

Roques, C., Weber, U. W., Brixel, B., Krietsch, H., Dutler, N., Brennwald, M. S., et al. (2020). In situ observation of helium and argon release during fluid-pressure-triggered rock deformation. *Scientific Reports*, *10*(1), 6949–6958. https://doi.org/10.1038/s41598-020-63458-x

Rorive, A., & Goderniaux, P. (2014). L'aquifère du Crétacé de la vallée de la Haine. In A. Dassargues, & K. Walraevens (Eds.), *Watervoerende lagen & gronwater in Belgie/Aquifères & eaux souterraines en Belgique* (pp. 183–190). Gent: Academia Press.

Sanford, W. E., Cook, P. G., & Dighton, J. C. (2002). Analysis of a vertical dipole tracer test in highly fractured rock. *Groundwater*, *40*(5), 535–542. https://doi.org/10.1111/j.1745-6584.2002.tb02538.x

Sanford, W. E., Shropshire, R. G., & Solomon, D. K. (1996). Dissolved gas tracers in groundwater: Simplified injection, sampling, and analysis. *Water Resources Research*, *32*(6), 1635–1642. https://doi.org/10.1029/96WR00599

Shakas, A., Linde, N., Baron, L., Selker, J., Gerard, M.-F., Lavenant, N., et al. (2017). Neutrally buoyant tracers in hydrogeophysics: Field demonstration in fractured rock. *Geophysical Research Letters*, *44*, 3663–3671. https://doi.org/10.1002/2017GL073368

Singhal, B. B. S., & Gupta, R. P. (2010). *Applied hydrogeology of fractured rocks*. Dordrecht, The Netherlands: Springer. https://doi.org/10.1007/978-90-481-8799-7

Skagius, K., & Neretnieks, I. (1986). Porosities and diffusivities of some nonsorbing species in crystalline rocks. *Water Resources Research*, *22*(3), 389–398. https://doi.org/10.1029/WR022i003p00389

Solomon, D. K., Cook, P. G., & Sanford, W. E. (1998). Chapter 9—Dissolved gases in subsurface hydrology. In C. Kendall, & J. J. McDonnell (Eds.), *Isotope tracers in catchment hydrology* (pp. 291–318). Amsterdam: Elsevier. https://doi.org/10.1016/B978-0-444-81546-0.50016-1

St. Clair, J., Moon, S., Holbrook, W. S., Perron, J. T., Riebe, C. S., Martel, S. J., et al. (2015). Geophysical imaging reveals topographic stress control of bedrock weathering. *Science*, *350*(6260), 534–538. https://doi.org/10.1126/science.aab2210

Tortell, P. D. (2005). Dissolved gas measurements in oceanic waters made by membrane inlet mass spectrometry: Oceanic gas measurements by MIMS. *Limnology and Oceanography: Methods*, *3*(1), 24–37. https://doi.org/10.4319/lom.2005.3.24

Tsang, C.-F., & Neretnieks, I. (1998). Flow channeling in heterogeneous fractured rocks. *Reviews of Geophysics*, *36*(2), 275–298. https://doi.org/10.1029/97RG03319

Tsang, Y. W. (1995). Study of alternative tracer tests in characterizing transport in fractured rocks. *Geophysical Research Letters*, *22*(11), 1421–1424. https://doi.org/10.1029/95GL01093

Van den Daele, G. F. A., Barker, J. A., Connell, L. D., Atkinson, T. C., Darling, W. G., & Cooper, J. D. (2007). Unsaturated flow and solute transport through the chalk: Tracer test and dual permeability modelling. *Journal of Hydrology*, *342*(1–2), 157–172. https://doi.org/10.1016/j.jhydrol.2007.05.021

Weatherill, D., Graf, T., Simmons, C. T., Cook, P. G., Therrien, R., & Reynolds, D. A. (2008). Discretizing the fracture-matrix interface to simulate solute transport. *Groundwater*, *46*(4), 606–615. https://doi.org/10.1111/j.1745-6584.2007.00430.x

Weede, M., & Hötzl, H. (2005). Strömung und transport in einer natürlichen Einzelkluft in poröser matrix—Experimente und ModellierungFlow and transport in a natural single fracture in a porous matrix—Experiments and modeling. *Grundwasser*, *10*(3), 137–145. https://doi.org/10.1007/s00767-005-0090-y